Enhanced heterogeneous nucleation on oxides in Al alloys by intensive shearing

# Enhanced heterogeneous nucleation on oxides in Al alloys by intensive shearing

**H T Li, Y Wang and Z Fan**
The EPSRC Centre-LiME, BCAST, Brunel University,
Uxbridge, Middlesex, UB8 3PH, United Kingdom

Email: mesrhhl@brunel.ac.uk

**Abstract.** Oxides, in liquid aluminium alloys, can cause severe difficulties during casting, contribute to the formation of cast defects and degrade the mechanical properties of cast components. In this paper, microstructural characteristics of naturally occurring oxides in the melts of commercial purity aluminium and Al-Mg binary alloys have been investigated. They are characterised by densely populated oxide particles within liquid oxide films. With intensive shearing, the particle agglomerates are dispersed into uniformly distributed individual particles. It was found that with intensive melt shearing, grain refinement of $\alpha$-Al can be achieved by the dispersed oxide particles. The smaller lattice misfit between the oxide particles and the $\alpha$-Al phase is characterised by a well defined crystallographic orientation relationship. And the mechanisms of grain refinement are discussed.

## 1. Introduction

Oxides are always present in liquid aluminium alloys and as more and more aluminium alloys are being recycled all over the world, more oxides can be accumulated, which presents an increasing challenge for the aluminium industry in terms of potential increased processing cost and decreased product quality [1, 2]. The presence of oxides affects casting process and causes degradation of mechanical properties of the final cast components and extensive efforts have been made to remove oxides from liquid aluminium alloys [3-5]. Recently, using melt conditioning by advanced shear technology (MCAST), it has been demonstrated that the naturally occurring oxides can be dispersed into uniformly distributed particles and therefore be less harmful to processing and resultant mechanical properties [6]. Moreover, it was found that the dispersed oxides can act as heterogeneous nucleation sites and a refined as-cast microstructure can be achieved [7-10]. In aluminium alloys, $\gamma$-$Al_2O_3$ and $\alpha$-$Al_2O_3$ are naturally occurring oxides depending on melting temperature and other conditions [11]. In AlMg alloys, either $MgAl_2O_4$ or MgO can be present in alloy melts, depending on the magnesium content, melting temperature and time at the melting temperature [12]. Both $MgAl_2O_4$ and $\alpha$-Al have a face-centred cubic (fcc) crystal structure, which could potentially enhance the heterogeneous nucleation of the fcc $\alpha$-Al phase to achieve refined microstructures. The objective of the present study was to investigate the feasibility of grain refinement through enhanced heterogeneous nucleation on the oxides in commercial purity aluminium (denoted CP Al) containing 99.86wt.%Al and Al-Mg binary alloys, by examination of the morphological evolution, the

crystallographic characteristics and the distribution of oxides with intensive melt shearing. The mechanisms of the enhanced heterogeneous nucleation on oxides are also discussed.

## 2. Experimental

In order to investigate the oxides naturally formed in the melts of CP Al and Al-Mg binary alloys, the oxides were concentrated by means of a pressure filtration technique. Pressure filtration has been shown to be an effective means to collect oxides and other inclusions to facilitate further investigations [7-9, 13]. For the cases without shearing, the oxides were concentrated after isothermal holding at 700$^{\circ}$C for 4 h and for those with shearing, the melts were sheared at 700$^{\circ}$C for 60 s and then immediately pressure filtered. The metallographic sample for scanning electron microscopy (SEM) investigation was prepared by standard metallographic technique and the samples were examined using a Zeiss Supera 35 FEG microscope, also equipped with an EDS facility, operated at an accelerating voltage of 5-15 kV. For crystallographic orientation relationship determination, samples for transmission electron microscopy (TEM) were cut from the filtered samples of Al-0.7Mg alloy by punching 3 mm diameter discs from just above the ceramic filter used for pressure filtration, where the highest volume fraction of oxides had been collected. The discs were then mechanically thinned down to 70 µm and then ion beam thinned using a Gatan precision ion polishing system (PIPS) at an energy of 5.0 kV and an incident angle of 4~6°. TEM examination was performed using a JEOL 2000FX microscope equipped with EDS facility at an accelerating voltage of 200 kV.

The standard TP-1 test was adopted to cast samples for grain size assessment. The melting temperature was 750$^{\circ}$C. After homogenisation for 1h, the alloy melt at 750$^{\circ}$C was poured into the MCAST unit for intensive shearing. After being sheared for 60 s, the melt was directly cast into the TP-1 mould, which had been preheated at 350$^{\circ}$C for 2 h. In all cases, the shearing temperature was set at 700$^{\circ}$C, the rotation speed was 500 rpm and the shearing time was 60 s. For the cases without shearing, the alloy melts were air cooled from 750 to 700$^{\circ}$C before casting into the TP-1 mould.

## 3. Results

Due to the high affinity of aluminium for oxygen, oxide films are readily formed on the surface of liquid aluminium when it is exposed to an atmosphere containing oxygen. The crystal structure of the oxide formed in CP Al at 700$^{\circ}$C has been identified by XRD analysis [14]. At 700$^{\circ}$C, the dominant oxide formed in the CP Al melt are thin films of $\gamma$-Al$_2$O$_3$ (figure 1a). More detailed observation reveals that the oxide films of $\gamma$-Al$_2$O$_3$ consist of platelet-like particles. Figure 1b shows the dispersed $\gamma$-Al$_2$O$_3$ oxide particles after shearing at 700$^{\circ}$C.



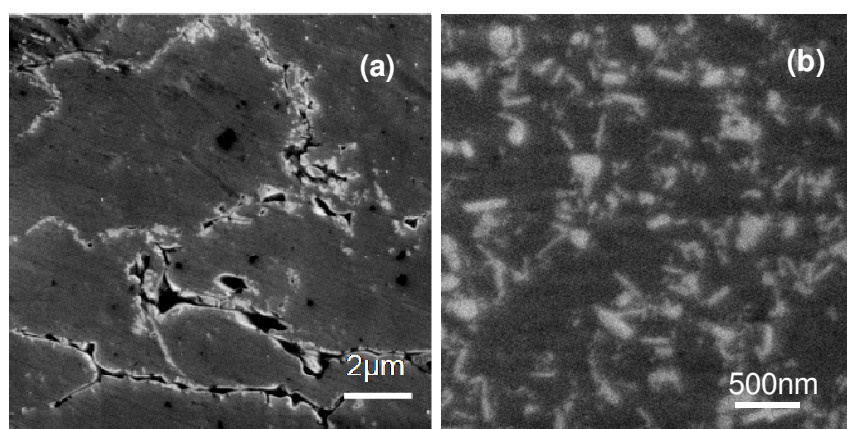**Figure 1.** SEM micrographs of $\gamma$-Al$_2$O$_3$ in the CP Al samples collected by pressure filtration technique at 700$^{\circ}$C, showing (a) oxide films in the non-sheared sample; (b) dispersed platelet-like oxide particles in the sheared sample.

Figure 2a shows the typical morphology of the oxides formed in the Al-0.7Mg alloy without melt shearing. The $MgAl_2O_4$ oxide formed in this alloy is in the form of oxide films, which have dense populations of $MgAl_2O_4$ particles within the oxide films. However, the $MgAl_2O_4$ particles in the Al-5Mg alloy are more discrete and no continuous oxide films are found (figure 2b). The $MgAl_2O_4$ particles in the Al-Mg alloys with a high Mg content (e.g. 5wt.%Mg) are dispersed naturally, even without the intensive melt shearing.
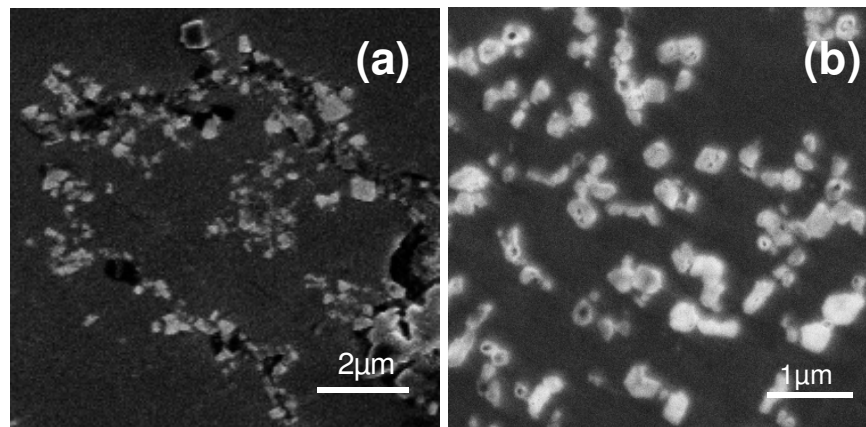


**Figure 2.** SEM micrographs of $MgAl_2O_4$ in the Al-Mg alloys at $700^oC$ with different magnesium contents without shearing, showing: (a) oxide films in the Al-0.7Mg alloy; (b) naturally dispersed $MgAl_2O_4$ particles in the Al-5Mg alloy.

TEM examination confirmed that the $MgAl_2O_4$ particles have {111} planes as their naturally exposed surface. More importantly, figure 3 provides the evidence of a cube-on-cube orientation relationship (OR) between the $MgAl_2O_4$ and the α-Al phases. The identified orientation relationship is:

$$(111)[110]\ MgAl_2O_4\ //\ (111)\ [110]\ \alpha\text{-Al} \tag{1}$$

This is very much as expected since both the $MgAl_2O_4$ and the α-Al phases have the same crystal structure and closely matched atomic spacings along the close packed directions on the close packed planes.
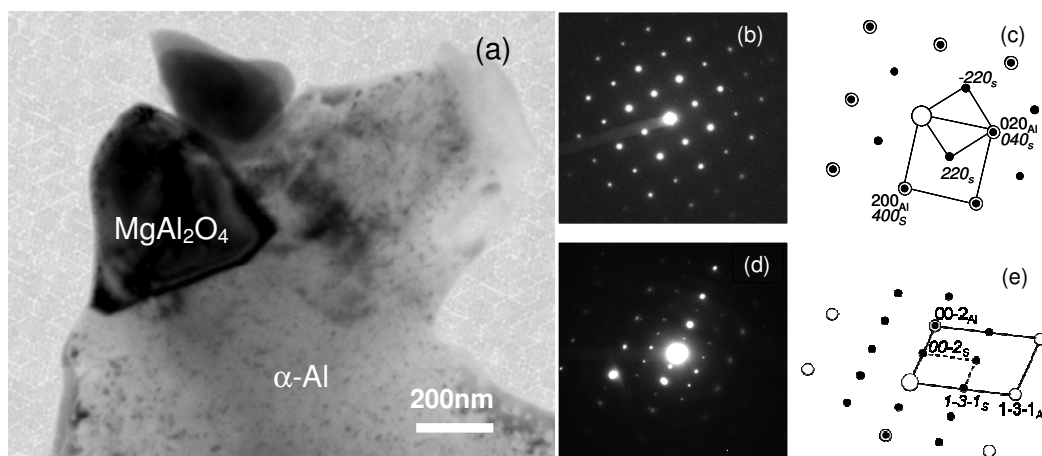


**Figure 3.** A bright field TEM micrograph and two SAD patterns showing the cube-on-cube crystallographic orientation relationship between the $MgAl_2O_4$ and α-Al phases. (a) A bright field TEM image showing the interface between $MgAl_2O_4$/α-Al; (b) SAD pattern with [001] zone axis; (c) indexed [001] pattern; (d) SAD pattern with [310] zone axis and (e) indexed [310] pattern.

The dispersed oxide particles developed by intensive melt shearing are expected to act as heterogeneous nucleation sites of the α-Al phase. The influence of intensive shearing on the grain refinement of the α-Al was investigated for the TP-1 samples of CP Al at 680°C. The macrographs of the longitudinal sections of the TP-1 samples are shown in Figure 4. The non-sheared sample exhibits a coarse columnar structure (figure 4a); in contrast, the sheared sample obtained at the same temperature, has a fine equiaxed grain structure (figure 4b).
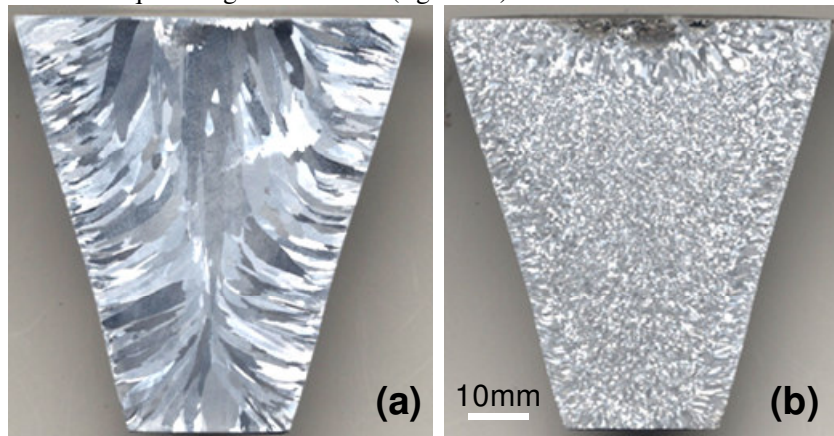


**Figure 4.** Macrographs of the TP-1 samples of CP Al showing the grain refinement of intensive melt shearing at 680°C: (a) coarse columnar grains of the non-sheared sample; (b) fine equiaxed grains of the sheared sample.

Figure 5 compares the grain structures of the Al-0.7Mg alloy samples obtained with and without intensive melt shearing, based on the longitudinal sections of the TP-1 samples. Without shearing, the Al-0.7Mg alloy, has a coarse columnar structure (figure 5a); whereas, after shearing, the grain structure was changed to a fine equiaxed structure (figure 5b). The grain size measurements for the TP-1 samples of both the CP Al and Al-0.7Mg alloys are compared in figure 6. With intensive melt shearing, the grain size of the CP Al was decreased from 1100 µm without shearing to 379 µm with shearing; for the Al-0.7Mg alloy, the grain size was decreased from 569 µm without shearing down to 221 µm with shearing. This clearly demonstrates that the grain size of both CP Al and Al-0.7Mg alloy can be refined by intensive melt shearing.
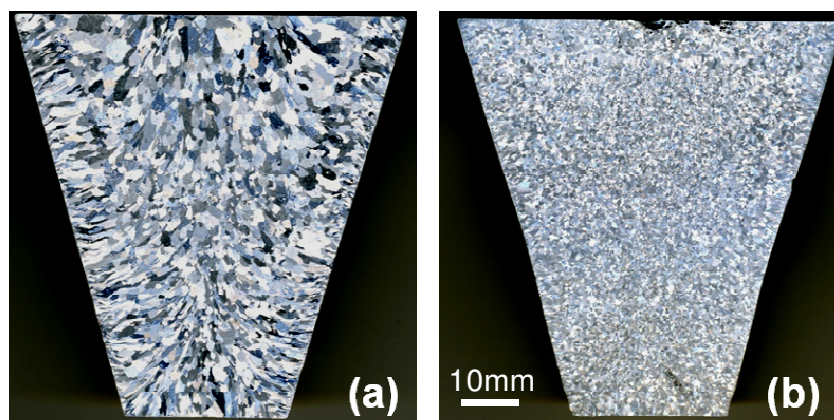


**Figure 5.** Macrographs of the TP-1 samples of Al-0.7Mg alloy showing the grain refinement of intensive melt shearing at 700°C: (a) coarse columnar grains of the non-sheared sample; (b) fine equiaxed grains of the sheared sample.
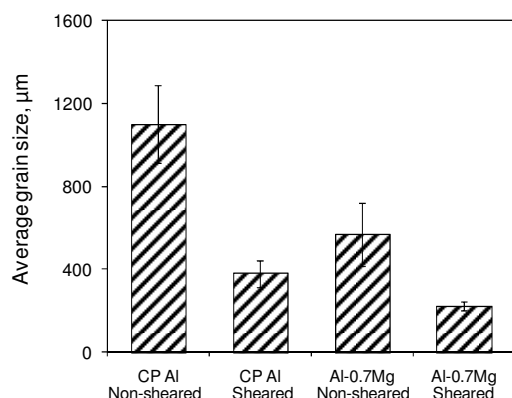
**Figure 6.** Comparisons of grain sizes of the TP-1 samples of CP Al and Al-0.7Mg alloys, showing the grain refining effects of intensive melt shearing.

## 4. Discussion

Oxide films naturally formed in liquid aluminium alloys consist of linear continuous films densely populated with oxide particles (figure 1a and figure 2a). With intensive melt shearing, these films can be dispersed so that individual oxide particles are uniformly distributed throughout the entire volume of liquid alloys (figure 1b). Alternatively, at an increased magnesium content, the continuous films are naturally dispersed (figure 2b).

TEM investigations have confirmed the availability of the close packed planes as the exposed surface of the naturally occurring $MgAl_2O_4$ oxides in Al-Mg alloys. The availability of the close packed planes in the naturally occurring oxides of $\gamma$-$Al_2O_3$ in CP Al has also been identified [14]. Table 1 compares the calculated lattice misfit between the oxides and the $\alpha$-Al phase in aluminium alloys on particular crystallographic planes (close packed planes) and directions. It is generally accepted that a necessary condition for a solid particle to be a potent heterogeneous nucleation site is the formation of a low energy interface between the solid nucleating particle and the nucleated phase, i.e., a coherent or at least a semicoherent interface with a small lattice misfit along the interface. This means the existence of a specific crystalline orientation relationship (OR) between the potent nucleating particle and the nucleated solid phase [13]. From Table 1, the smaller lattice misfit ($f_0$) between the oxides and the $\alpha$-Al phase implies a high potency of the oxide particles, either $MgAl_2O_4$ or $\gamma$-$Al_2O_3$, as nucleation sites of the $\alpha$-Al phase.

**Table 1.** Calculated lattice misfit ($f_0$) between the oxides and the $\alpha$-Al phase at 660$^{\circ}$C.

| Interface S/N | Crystal structure & Lattice parameters, nm | OR: $(hkl)[uvw]_N$// $(hkl)[uvw]_S$ | $d_S$, nm | $d_N$ nm | $f_0$ (%) |
|---|---|---|---|---|---|
| $MgAl_2O_4$/$\alpha$-Al | S: fcc, a=0.81263, N: fcc, a=0.41212 | (111)[110]// (111)[110] | 0.57462 | 2×0.29141 | **1.41** |
| $\gamma$-$Al_2O_3$/$\alpha$-Al | S:fcc, a=0.79634, N: fcc, a=0.41212 | (111)[110]// (111)[110] | 0.56310 | 2×0.29141 | **3.38** |

To achieve grain refinement of the $\alpha$-Al phase by enhanced heterogeneous nucleation on inoculants, spatially dispersed grain refiner particles with high nucleation potency throughout the bulk melt are necessary and either settling or agglomeration behaviour of the grain refiner particles should be avoided. In other words, the existence of potent nucleating agents may not necessarily lead to grain

refinement in the solidified microstructure. In line with the free growth model, for effective grain refinement of a given alloy composition, the potent nucleating particles need to have a sufficient number density and a favourable particle size and size distribution [15]. The theoretical modelling by Men et al. using the free growth model revealed quantitatively that intensive melt shearing can effectively disperse oxide particles formed on continuous oxide films into more individual particles in the alloy melt, resulting in an increase in the oxide particle density by three orders of magnitude [8]. In the present work, dispersed oxide particles by intensive melt shearing provided a sufficient density of individual oxide particles to enhance the heterogeneous nucleation of the $\alpha$-Al phase in both CP Al and Al-0.7Mg alloy.

## 5. Conclusions
(1) The oxide naturally occurring in liquid CP Al is $\gamma$-$Al_2O_3$. The oxide formed in Al-Mg alloys is $MgAl_2O_4$. Dense populations of these oxide particles are formed within the continuous liquid oxide films or clusters.
(2) The small lattice misfit between the naturally occurring oxides and the $\alpha$-Al phase on close packed crystallographic planes and directions means that the oxides formed in liquid aluminium alloys are potent nucleation sites for the $\alpha$-Al phase.
(3) Intensive melt shearing disperses oxide particles within oxide films or clusters into individual oxide particles uniformly distributed throughout the entire volume of liquid Al alloys.
(4) Intensive melt shearing enhances the heterogeneous nucleation of the $\alpha$-Al phase on the dispersed oxide particles through the increased number density of the individual oxide particles and therefore refines the grains of the $\alpha$-Al phase.

**References**
[1]  Sabatino M D, Arnberg L, Rørvik S and Prestmo A 2005 *Mater. Sci. Eng.* A **413-414** 272-6
[2]  Timelli G and Bonollo F 2007 *Int J Cast Metal Res* **20** 304-11
[3]  Davis J R 1993 Molten aluminium processing and casting. *ASM speciality handbook.* pp. 199-230.
[4]  Sigworth G K, Shivkumar S and Apelian D 1989 *AFS Trans.* **139** 811-24
[5]  Cao X and Campbell J 2003 *Metall. Mater. Trans.* A **34** 1409-20
[6]  Tzamtzis S, Zhang H, Xia M, Babu N H and Fan Z 2011 *Mater. Sci. Eng.* A **528** 2664-9
[7]  Fan Z, Wang Y, Xia M and Arumuganathar S 2009 *Acta Mater.* **57** 4891-901
[8]  Men H, Jiang B and Fan Z 2010 *Acta Mater.* **58** 6526
[9]  Li H T, Xia M, Jarry Ph, Scamans G M and Fan Z 2011 *J. Cryst. Growth* **314** 285-92
[10] Zuo Y, Li H, Xia M, Jiang B, Scamans G M and Fan Z 2011 *Scripta Mater.* **64** 209-12
[11] Impey S A, Stephenson D J and Nicholls J R 1988 *Mater. Sci. Tech.* **4** 1126-32
[12] Cochran C N, Belitskus D L and Kinosz D L 1977 *Metall. Trans.* B **8** 323-32
[13] Wang Y, Xia M, Fan Z, Zhou X and Thompson G E 2010 *Intermetallics* **18** 1683-9
[14] Li H T 2011 PhD thesis (London: Brunel University) p 174
[15] Greer A L, Bunn A M, Tronche A, Evans P V and Bristow D J 2000 *Acta Mater.* **48** 2823-35